Full Paper

THERMAL ANALYSIS OF THE RIB EDGE TREATMENT IN INTERRUPTED MICROCHANNEL HEAT EXCHANGER

T.A. Alo
Department of Mechanical Engineering, Obafemi Awolowo University, Ile-Ife, Nigeria.

S. A. Adio
Department of Mechanical Engineering, Obafemi Awolowo University, Ile-Ife, Nigeria.
adiosa@oauife.edu.ng.

ABSTRACT

Solving the problem of effective heat dissipation is of importance in electronic systems and other portable systems. This is particularly important to maintain the system's efficiency and to increase the durability of the system's component parts. In this study, a three-dimensional interrupted microchannel is designed and modelled to study and verify the thermal performance of the microchannel heat sink for effective thermal management in a compact space. The performance of the microchannel heat sink is optimized by carrying out a three-dimensional edge treatment of different rib configurations to determine the best design that will improve the heat transfer capability of the heat sink. Nanofluids formulated from Al_2O_3 nanoparticle and water having different volume fraction is used as the working fluid. The influence of increasing the nanoparticle volume fraction and the Reynolds number on the performance of the heat sink was also studied. The Al_2O_3-water nanofluid showed improved thermal performance in the microchannel heat sink when compared with water. Increasing the Reynolds number increased both the heat transfer coefficient and the pressure drop within the system, however, the performance evaluation criteria showed that the increase in the heat transfer coefficient surpassed that of the pressure drop.

Keywords: Interrupted microchannel; rectangular rib; thermal performance; nanofluid; heat transfer enhancement.

1. INTRODUCTION

Heat dissipation is a key issue today and it's a major factor in ensuring rapid development and reliable operations of electronic components especially when designing with space constraints. A microchannel heat sink (MCHS) is believed to be an efficient available method to solve cooling problems in electronics and hence it is a widely adopted method of cooling in the electronics industry today. With the recent advancement in Nanotechnology, nanoparticles are also used to improve thermal efficiency in MCHS applications today. The nanofluids generally consist of nanoparticles and a base fluid (oil, water, glycol etc.) and when compared to water have proven to be more efficient and a few research work (numerical and experimental) have been conducted to validate this claim. Some of such investigations applied experimental methods (Lee et al., 2005 Garimella, & Liu, 2005; Sarafraz et al., 2017; Xu, 2000; Zhai et al., 2017) and numerical methods (Adewumi et al., 2016; Bello-Ochende et al., 2018; Kumar & Sarkar, 2018; Naqiuddin et al., 2018).

Tuckerman and Pease (1981) in their work introduced the use of microchannels and discovered its ability to dissipate a large amount of heat from the high density very-large-scale integrated circuit (VLSI). The numerical and experimental analysis of a single-phase MCHS was carried out by Qu and Muduwar (2002) in order to obtain the pressure drop and heat transfer characteristics of the heat sink. It was observed in their work, that the conventional Navier-Stokes equations and energy equations can adequately predict the fluid flow and heat transfer characteristics.

In macroscale heat transfer, Xu et al. (2005) in their work demonstrated a silicon microchannel and several transverse microchannels which separates the whole flow length into several zones. It was discovered that the computed hydraulic and thermal boundary layers were redeveloping in each separated zone due to shortened flow length for the interrupted microchannel heat sink.

A microchannel with staggered rectangular ribs in its transverse microchambers was studied by Chai and Wang (2018) Chai et al., (2016b) and Chai et al. (2013). This was done to improve the redeveloping thermal boundary layer effect already studied by Xu et al. (2015). Ribs were used to increase the convection heat transfer rate of the system and because of the ease in manufacturing. From the literatures above, one can safely say that interrupting the thermal boundary layer and inducing the separation at the mainstream are two efficient means to improve heat transfer in microscale applications or better still in a microchannel. Ijam & Saidur (2012), also used nanofluids as the coolant for a microchannel heat sink in their study. The results showed that silicon nanoparticles present a higher thermal conductivity when compared with titanium nanoparticles at the same volume fraction. However, there was no comparison of an adverse effect of the nanofluid with the microchannel used in this study.

Sharifpur et al. (2015) and Adio et al. (2016) in their work, presented the stability of nanofluids which brings about its higher performance in heat transfer and they also gave evidence that there is an increase in viscosity of this new fluid and this might affect the pumping requirement.

The objective of this study is to increase the overall efficiency of a microchannel by optimizing the shape of the rib at the microchamber which is applicable in electronic applications such as the Binder Jet printing, aerospace industry, etc. According to the

literatures reviewed, there are few detailed types of research on the thermal performance of MCHS with nanofluids. Nevertheless, to the best of the authors' knowledge, there is no numerical assessment of rib edge treatments using a nanofluid as the coolant. This paper reports an optimization action by considering two rib configurations, at different volume fractions and at different Reynolds number (Re). The effects of volume fraction and Re on the thermal performance of this heat sink are presented too.

2. MATERIALS AND METHODS

2.1. Computational domain and boundary conditions:

For this study, an interrupted microchannel (Figure 1) is employed following the methodology of Chai et al. (2013) and the computational domain adopted is based on the spanwise symmetry and periodic boundaries assumptions as shown in Figure 2. The geometric parameters in the figure are shown in Table 1 and the computational domain (denoted as IMCH-R) would serve as the reference model for comparison and validation. Rib edge treatment is an optimization process, whereby additional features are added to the rib to optimize heat transfer properties of the microchannel. The rib is then treated by adding a fillet (IMCH-FL) and a chamfer (IMCH-CF) of a radius of 0.04 mm as shown in Figure 3. The cooling medium used in this study is a nanofluid of aluminium-oxide nanoparticles and water (Qi et al., 2017). The nanofluid was considered based on its effective heat transfer properties as studied by Shi et al. (2018). To evaluate the thermal performance of this nanofluid, an assumption that the aluminium-oxide nanoparticles and water are in thermal equilibrium was made. Other assumptions are; there is no energy generation in the fluid, incompressible flow, steady-state laminar flow and dependency of volume fraction on temperature.

Due to these assumptions, the governing equations are:

The continuity equation:

$$\nabla.\left(\rho_{nf}\,\vec{u}\right)=0 \tag{1}$$

The momentum equation:

$$\nabla.\left(\rho_{nf}\vec{u}\vec{u}\right)=-\nabla p+\nabla.\left(\mu_{nf}\nabla\vec{u}\right) \tag{2}$$

Table 1: The dimension of the Microchannel heat sink

Parameter	Dimension (mm)
L(a)	20
W	2.5
h	0.35
T	0.1
L(b)	10
K	1.1
rl	0.4
w	0.25
H	0.35

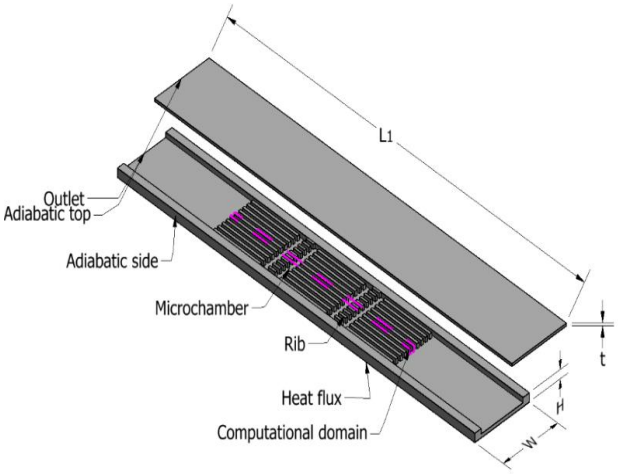

Figure 1: Interrupted Microchannel Heat Sink

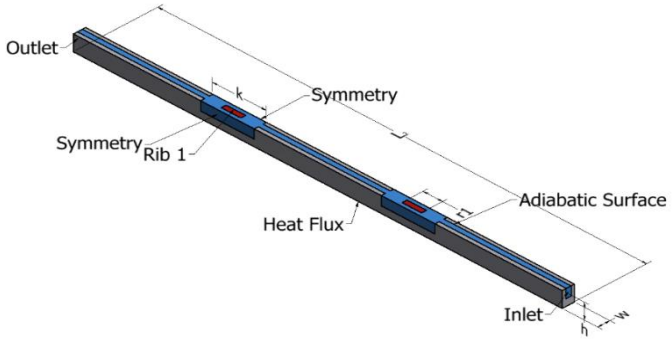

Figure 2: Computational domain of the interrupted microchannel heat sink (IMCH-R)

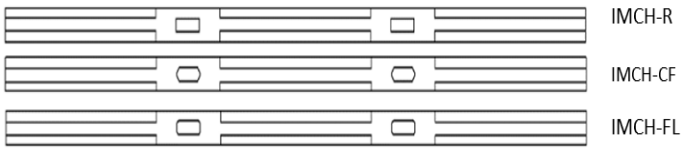

Figure 3: The different rib configurations used in this study

The energy equation for the fluid region:

$$\nabla.\left(\rho_{nf}\vec{u}c_{p,nf}T\right)=\nabla.\left(k_{nf}\nabla T\right) \tag{3}$$

The energy equation for the solid body:

$$\nabla.\left(k_s\nabla T_s\right)=0 \tag{4}$$

The single-phase model (Bahiraei & Alighardashi, 2016) employed for the density, heat capacity, viscosity and thermal conductivity of the nanofluid was used based on the above-listed assumptions and a user-defined function was used to input these properties into the CFD solver. The properties are as follows:

$$\rho_{nf}=(1-\varphi)\rho_f+\varphi\rho_p \tag{5}$$

$$c_{p,nf}=\frac{(1-\varphi)\rho_f c_{p,f}+\varphi\rho_p c_{p,p}}{\rho_{nf}} \tag{6}$$

$$\mu_{nf}=\mu_{static}+\mu_{dynamic} \tag{7}$$

$$k_{nf}=k_{static}+k_{dynamic} \tag{8}$$

The static thermal conductivity (k_{static}) and the dynamic thermal conductivity ($k_{dynamic}$) of the nanofluid (Hamilton & Crosser, 1962) is given as:

$$k_{static} = k_f \left\{ \frac{(k_p+2k_f)-2\varphi(k_f-k_p)}{(k_p+2k_f)+\varphi(k_f-k_p)} \right\} \quad (9)$$

$$k_{dynamic} = 5 * 10^4 \varphi \rho_f c_{pf} \sqrt{\frac{K_b T}{d_p \rho_p}} g(T,\varphi) \quad (10)$$

The "g function" ($g(T,\varphi)$) in the equation above is given as:

$$g(T,\varphi) = (a + bln(dp) + cln(\varphi) + dln(\varphi)\,ln(dp) + eln(dp)^2)\,ln(T) + (m + hln(dp) + iln(\varphi) + jln(\varphi)\,ln(dp) + kln(dp)^2) \quad (11)$$

The value of the constants in the above equation has been determined semi-empirically and are given in Table 2 based on the work of Jang a& Choi (2013).

The dynamic viscosity and static viscosity were calculated from the equations below:

$$\mu_{static} = \frac{\mu_f}{(1-\varphi)^{2.5}} \quad (12)$$

$$\mu_{dynamic} = 5 * 10^4 \varphi \rho_f \sqrt{\frac{K_b T}{d_p \rho_p}} g(T,\varphi) \quad (13)$$

Where the "g function" ($g(T,\varphi)$) is the same as earlier stated.

2.2. Validation of Numerical Models:

In order to validate and ensure the accuracy of the numerical simulation, the validation of the numerical code was conducted against the experimental results of Chai et al. (2013) for IMCH-R with a rib length of 0.4mm using water as the working fluid. The maximum deviation of numerical f_{ave} from experimental results is less than 5% as shown in Figure 4.

The mesh independence analysis is performed using several different meshes with a smaller element size near the walls for every microchannel heat sink. A Reynolds number of 441 is considered and the Al_2O_3-water nanofluid is used as the working fluid in this grid independent study. For the IMCH-R, the deviations of the average friction factor (f_{ave}) using 0.369, 0.507, 0.708 million grids from that of 1.192 million grids are 4.35%, 0.04%, 0.12% respectively. Therefore the 0.507 million grid is used and the same technique was used to determine grid points for every microchannel heat sink studied in this research. The 0.572 and 0.688 million grids are respectively used for IMCH-FL and IMCH-CF.

Table 2: The g-function constant values.

Constant	Values
a	52.81348876
b	6.115637295
c	0.695574508
d	4.17E-02
e	0.1769193
m	-298.1981908
h	-34.53271691
i	-3.922528928
j	-0.235432963
k	-0.999063481

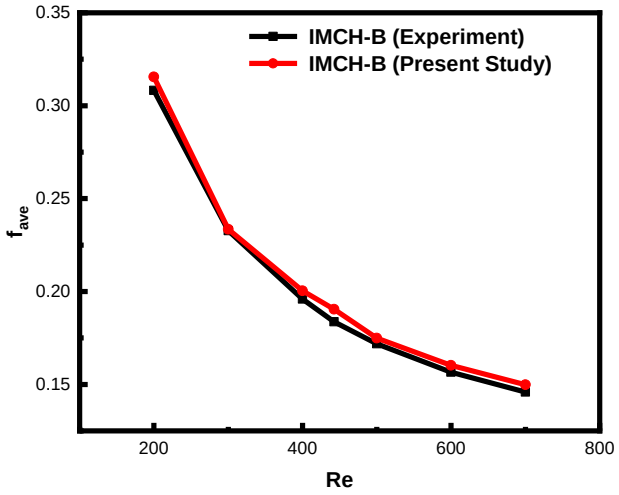

Figure 4: Friction factor comparison of present numerical result with experimental data of Chai et al. (2013)

2.3. Boundary conditions:

A uniform heat flux of $122\ W/cm^2$ is imposed at the bottom wall of the microchannel, to typify the amount of heat observed in complex computer systems today. The temperature at the inlet of the microchannel is taken to be 293 K. The external walls are assumed adiabatic with no convection or radiation heat transfer with the surrounding environment. The nanofluid enters the inlet with an initial velocity, $\vec{u}_0$ and exits the outlet at the atmospheric pressure, p_0. On all the conjugate surfaces, a no-slip boundary condition is imposed.

2.4. Processing of Results:

The physics of the present problem was set up using a commercially licensed ANSYS FLUENT®. The momentum and the energy equations were solved employing the second-order upwind scheme while the governing equations with the associated boundary conditions were discretized and solved using the finite volume method. The pressure and the velocity fields were coupled using the SIMPLEC algorithm. The accuracy of the solution to convergence was monitored at 10^{-6} for the continuity, velocity and 2×10^{-8} for the energy equation. The following evaluation criteria are defined to quantitatively determine the thermal performance of the heat sink. They are:

$$Re = \frac{\rho_f u_m D_h}{\mu_f} \quad (14)$$

Where, ρ_f is the average density of the fluid, u_m is the average velocity of the flow and μ is the average dynamic viscosity. The local convective heat transfer coefficient (h_x) is defined as:

$$h_x = \frac{q''(LW)}{NA_C(T_w - T_f)} \quad (15)$$

where, q'' is the heat flux, N represents the number of channels, A_C is the contact surface area available for heat transfer, D_h is the hydraulic diameter, T_w is the average temperature of the wall and T_f is the local bulk fluid temperature obtained from Chai et al. (2016a).

The average heat transfer coefficient is then given as

$$h_{ave} = \frac{1}{L}\int h_x dx \quad (16)$$

The performance criteria of the heat sink is of interest and this includes the monitoring of the pumping power requirement of the heat sink vis à vis the nanofluid that is employed. The pumping power is defined as:

$$P_{pump} = \dot{Q}\Delta p \quad (17)$$

where $\dot{Q}$ is the volumetric flow rate of the nanofluid. The performance evaluation criterion (PEC) is used to evaluate the performance of the heat sink as a function of its thermal performance and pumping cost. It is defined as:

$$PEC = \frac{h_{nf}/h_{bf}}{\Delta p_{nf}/\Delta p_{bf}} \quad (18)$$

The thermal enhancement factor, ɳ is defined as the ratio of the relative heat transfer coefficient to the relative pressure drop under similar operating conditions (i.e. similar Re and φ):

$$ɳ = \frac{h/h_0}{\Delta p/\Delta p_0}\Big|_{\varphi} \quad (19)$$

3. RESULTS AND DISCUSSION

The mixture of aluminium-oxide nanoparticles and water is studied numerically as it flows through the microchannel and its heat transfer properties are reported in comparison with water to determine the most efficient cooling medium. Figure 5 shows the average heat transfer coefficient of water and that of the nanofluid at different volume fractions of the IMCH-R. As can be seen, the heat transfer coefficient of the nanofluids increased at a range of 9-13%, which shows that there is an increase in the nanofluid's thermal conductivity when compared with water. It can be seen that the heat transfer performance increases with the increase in Reynolds number under the same nanofluid concentration condition and the magnification of heat transfer do not increase linearly with increase in nanoparticle concentration. It can then be concluded that the nanofluid enhances heat transfer and this depends on the thermal properties and also the interactions between the nanoparticle and the base fluid.

The thermal performances of the new heat sinks with different edge treatment and nanofluid concentration are studied by taking into consideration the performance evaluation criteria (PEC) as described earlier. The PEC shows that the heat transfer enhancement is larger than the pressure drop increase and consequently its energy saving. The PEC of the new microchannels (IMCH-FL and IMCH-CF) is greater than unity in all cases which shows an increase in pressure. This further enhances the performance of the microchannel heat sink. As shown in Figure 6, with an increase of Re number, the performance evaluation criteria of the new microchannels (IMCH-FL and IMCH-CF) increases.

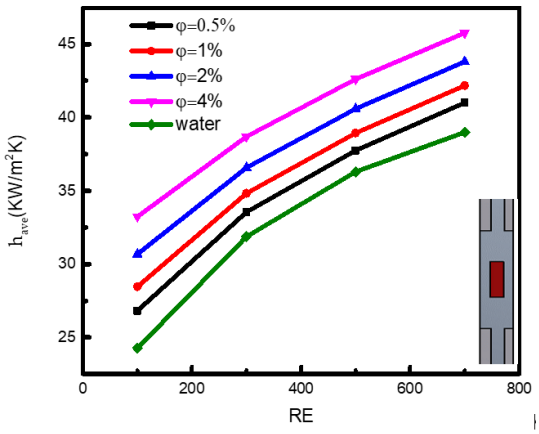

Figure 5: Average heat transfer coefficients of the nanofluids and water at different Reynolds numbers

Furthermore, with an increase in φ , the PEC increases and then reduces at a fixed value. The heat transfer enhancement of the observed microchannels is suitable to the condition at φ‹ 2% having its maximum at 2%. For φ›2%, the PEC dropped to the working condition slightly above that of the nanofluid with 0.5% this is because the rate of pressure drop increased more than heat transfer rate as a result of higher viscosity value at φ›2% particle concentration. The IMCH-FL in this study has proven to be the best due to its PEC (45.9%) being the highest at Re 300 and $\varphi = 2\%$. This implies that in the design of an interrupted microchannel with ribs described in this study, the configuration at the optimum operation scope is the IMCH- FL. The performance of the microchannel heat sinks based on the thermal enhancement factor (ɳ) as defined by Eq. (19) The level of improvement in the performance of the interrupted microchannel is studied by this factor and reported in Figure 7 below. It can be seen that the IMCH-FL showed the best performance at 15.84% for 2% concentration and Reynolds number of 700.

Also, the PEC described earlier also buttress the fact that IMCH-FL has the best thermal performance which is the same as what the thermal enhancement factor has shown which is more than unity (i.e. it still outperformed the reference microchannel, IMCH-R).

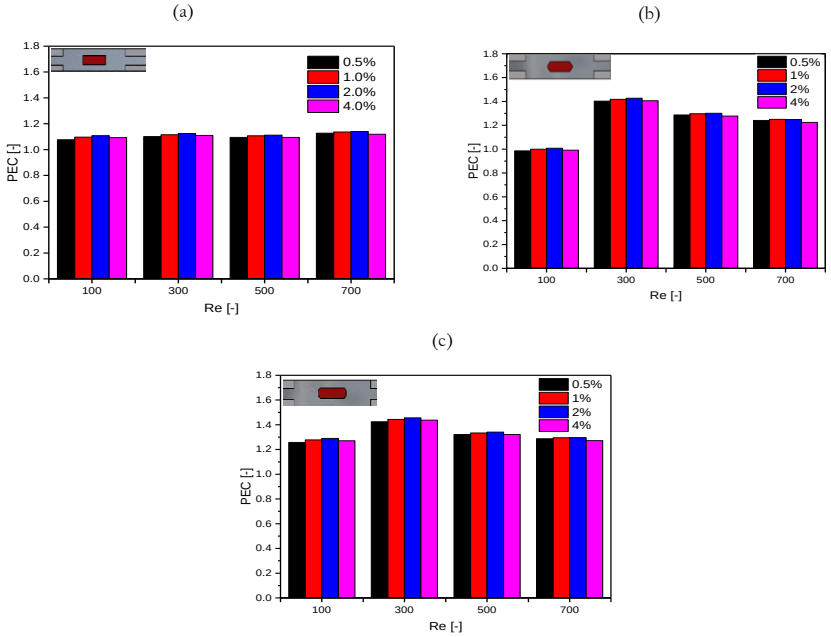

Figure 6: Variation of PEC with Re, φ parameter and different rib configurations used in this study

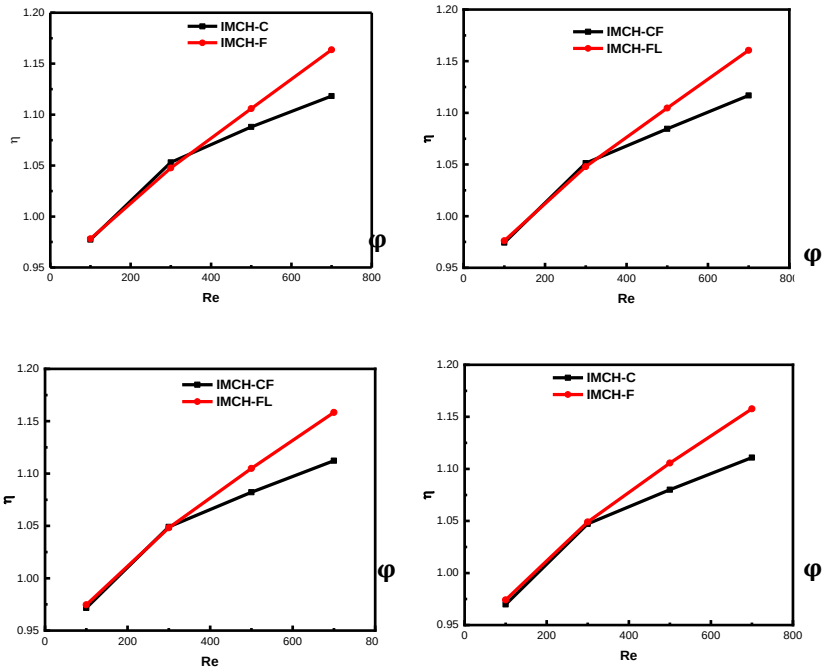

Figure 7: Variation of PEC with Re, φ parameter and different rib configurations used in this study

4. CONCLUSION

In this study, the thermal analysis of Al_2O_3-water nanofluids in interrupted microchannel heat sinks having ribs in its microchamber was studied. The results show that the use of the nanofluid in the interrupted microchannel that is equipped with edge-treated rectangular ribs improves the thermal performance of the heat sink. In this study, it was concluded that the use of Al_2O_3-water nanofluid in place of pure water showed substantial and outstanding improvement in the thermal performance of the heat sink.

The performance evaluation criteria showed that the use of Al_2O_3-water is better than pure water in the heat sinks taken into consideration the increase in pressure as a function of heat dissipation.

Treating the ribs of the interrupted microchannel has proven to be advantageous in enhancing the thermal performance of the heat sink and when comparing the results of the edge treated configurations with the reference heat sink having rectangular rib the IMCH-F is the best configuration due to parameters investigated.

REFERENCES

Adewumi, O., Bello-Ochende, T., & Meyer, J. Constructal Design of Single Microchannel Heat Sink With Varying Axial Length and Temperature-Dependent Fluid Properties. *International Journal of Heat and Technology*, *34*(Special Issue 1), S167–S172, 2016.

Adio, S. A., Mehrabi, M., Sharifpur, M., & Meyer, J. P. Experimental investigation and model development for effective viscosity of MgO-ethylene glycol nanofluids by using dimensional analysis, FCM-ANFIS and GA-PNN techniques. *International Communications in Heat and Mass Transfer*, *72*, 71–83, 2016.

Bahiraei, M., & Alighardashi, M. Investigating non-Newtonian nanofluid flow in a narrow annulus based on second law of thermodynamics. *Journal of Molecular Liquids*, *219*, 117–127, 2016.

Bello-Ochende, T., Meyer, J. P., & Ighalo, F. U. Combined numerical optimization and constructal theory for the design of microchannel heat sinks. *Numerical Heat Transfer; Part A: Applications*, *58*(11), 882–899, 2010.

Chai, L., & Wang, L. Thermal-hydraulic performance of interrupted microchannel heat sinks with different rib geometries in transverse microchambers. *International Journal of Thermal Sciences*, *127*(January), 201–212, 2018.

Chai, L., Xia, G. D., & Wang, H. S. (a). Laminar flow and heat transfer characteristics of interrupted microchannel heat sink with ribs in the transverse microchambers. *International Journal of Thermal Sciences*, *110*, 1–11, 2016.

Chai, L., Xia, G. D., & Wang, H. S. (b). Parametric study on thermal and hydraulic characteristics of laminar flow in microchannel heat sink with fan-shaped ribs on sidewalls - Part 2: Pressure drop. *International Journal of Heat and Mass Transfer*, *97*, 1081–1090, 2016.

Chai, L., Xia, G., Zhou, M., Li, J., & Qi, J. Optimum thermal design of interrupted microchannel heat sink with rectangular ribs in the transverse microchambers. *Applied Thermal Engineering*, *51*(1–2), 880–889, 2013.

Hamilton, R., & Crosser, O. Thermal conductivity of heterogeneous two-component systems. *Industrial & Engineering Chemistry ...*, *1*, 187–191, 1962.

Ijam, A., & Saidur, R. Nanofluid as a coolant for electronic devices (cooling of electronic devices). *Applied Thermal Engineering*, *32*, 76–82, 2012.

Jang, S. P., & Choi, S. U. S. *Effects of Various Parameters on Nanofluid Thermal Conductivity*. *129*(May 2007), 2013.

Jia, Y., Xia, G., Li, Y., Ma, D., & Cai, B. Heat transfer and fluid flow characteristics of combined microchannel with cone-shaped micro pin fins. *International Communications in Heat and Mass Transfer*, *92*, 78–89, 2018.

Kumar, V., & Sarkar, J. Two-phase numerical simulation of hybrid nanofluid heat transfer in minichannel heat sink and experimental validation. *International Communications in Heat and Mass Transfer*, *91*, 239–247, 2018.

Lee, P.-S., Garimella, S. V., & Liu, D. Investigation of heat transfer in rectangular microchannels. *International Journal of Heat and Mass Transfer*, *48*(9), 1688–1704, 2005.

Naqiuddin, N. H., Saw, L. H., Yew, M. C., Yusof, F., Ng, T. C., & Yew, M. K. Overview of micro-channel design for high heat flux

application. *Renewable and Sustainable Energy Reviews*, *82*(June 2017), 901–914, 2018.

Qi, C., Hu, J., Liu, M., Guo, L., & Rao, Z. Experimental study on thermo-hydraulic performances of CPU cooled by nanofluids. *Energy Conversion and Management*, *153*(July), 557–565, 2017.

Qu, W. and Mudawar, I. Experimental and numerical study of pressure drop and heat transfer in a single-phase micro-channel heat sink. *International Journal of Heat and Mass Transfer*, *45(12)*, 2549–2565, 2002.

Sarafraz, M. M., Arya, A., Hormozi, F., & Nikkhah, V. On the convective thermal performance of a CPU cooler working with liquid gallium and CuO/water nanofluid: A comparative study. *Applied Thermal Engineering*, *112*, 1373–1381, 2017.

Sharifpur, M., Adio, S. A., & Meyer, J. P. Experimental investigation and model development for effective viscosity of Al2O3-glycerol nanofluids by using dimensional analysis and GMDH-NN methods. *International Communications in Heat and Mass Transfer*, *68*, 2015.

Shi, X., Li, S., Wei, Y., & Gao, J. Numerical investigation of laminar convective heat transfer and pressure drop of water-based Al2O3nanofluids in a microchannel. *International Communications in Heat and Mass Transfer*, *90*, 111–120, 2018.

Tuckerman, D. B., & Pease, R. F. W. *High-Performance Heat Sinking for VLSI*. (5), 126–129, 1981.

Xu, B., Ooti, K. T., Wong, N. T., & Choi, W. K. Experimental investigation of flow friction for liquid flow in microchannels. *International Communications in Heat and Mass Transfer*, *27*(8), 1165–1176, 2000.

Xu, J. L., Gan, Y. H., Zhang, D. C., & Li, X. H. Microscale heat transfer enhancement using thermal boundary layer redeveloping concept. *International Journal of Heat and Mass Transfer*, *48*(9), 1662–1674, 2005.

Zhai, Y., Xia, G., Li, Z., & Wang, H. Experimental investigation and empirical correlations of single and laminar convective heat transfer in microchannel heat sinks. *Experimental Thermal and Fluid Science*, *83*, 207–214, 2017.